Gutman, M., & Nachliel, E. (1985) *Biochemistry* (following paper in this issue).
Gutman, M., Huppert, D., & Pines, E. (1981) *J. Am. Chem. Soc. 103*, 3709–3717.
Gutman, M., Nachliel, E., Gershon, E., & Giniger, R. (1983a) *Eur. J. Biochem. 134*, 63–69.
Gutman, M., Nachliel, E., Gershon, E., Giniger, R., & Pines, E. (1983b) *J. Am. Chem. Soc. 105*, 2210–2216.
June, D. S., Saelter, C. H., & Dye, J. L. (1981) *Biochemistry 20*, 2707–2719.
MacKnight, M. L., Gillard, J. M., & Tollin, G. (1973) *Biochemistry 12*, 4200–4206.
March, K. L., Maskalik, G. D., England, R. D., Friend, S. H., & Gurd, F. R. N. (1982) *Biochemistry 21*, 5241–5251.
Mathew, J. B., Hanania, G. I. H., & Gurd, F. R. N. (1981) *Biochemistry 20*, 571–580.
Nachliel, E., & Gutman, M. (1984) *Eur. J. Biochem. 143*, 83–89.
Shire, S. J., Hanania, G. I. H., & Gurd, F. R. N. (1974a) *Biochemistry 13*, 2967–2974.
Shire, S. J., Hanania, G. I. H., & Gurd, F. R. N. (1974b) *Biochemistry 13*, 2974–2979.
Shire, S. J., Hanania, G. I. H., & Gurd, F. R. N. (1975) *Biochemistry 14*, 1352–1358.
Silvestrini, M. C., Burnori, M., Wilson, M. T., & Darly-Usmar, V. M. (1981) *J. Inorg. Biochem. 14*, 327–338.
Tanford, C. (1976) *Physical Chemistry of Macromolecules*, Wiley, New York.

Kinetic Analysis of Protonation of a Specific Site on a Buffered Surface of a Macromolecular Body†

Menachem Gutman* and Esther Nachliel
Department of Biochemistry, Tel Aviv University, Tel Aviv, Israel
Received June 22, 1984; Revised Manuscript Received November 2, 1984

ABSTRACT: The kinetics of protonation of a specific site on a macromolecular structure (micelle) in buffered solution was studied with the purpose of evaluating the effect of buffer on the observed dynamics. The experimental system consisted of the following elements: Brij 58 micelles serving as homogeneous uncharged macromolecular bodies, bromocresol green, a well-adsorbed proton detector, and 2-naphthol-3,6-disulfonate as a proton emitter in the bulk. Imidazole was the mobile buffer while neutral red, which has a high affinity for the micellar surface, served as the immobile buffer. An intensive laser pulse ejects a proton from the proton emitter, and the subsequent proton-transfer reactions are measured by fast spectrophotometric methods. The dynamics of proton pulse in buffered solution are characterized by a very rapid trapping of the discharged protons by the abundant buffer molecules. This event has a major effect on the kinetic regime of the reaction. During the first 200 ns the proton flux is rate limited by free-proton diffusion. After this period, when the free-proton concentration decayed to the equilibrium level, the relaxation of the system is carried out by the diffusion of buffer. Thus in the buffered biochemical system, at neutral pH, most of proton flux between active sites and bulk is carried out by buffer molecules—not by diffusion of free protons. Surface groups on a high molecular weight body exchange protons among them at a very fast rate. This reaction has a major role on proton transfer from a specific site to the bulk. The proton can reach the bulk either through dissociation—diffusion or through collisional proton transfer between the mobile buffer and protonable surface groups. The rapid proton exchange between the surface groups increases the efficiency of the latter pathway. It is proposed that a combination of free proton diffusion and buffer-mediated proton diffusion can generate an apparent asymmetry in the "bulk to surface" vs. "surface to bulk" proton transfer. Low-pK surface groups will mostly enhance the rate of proton transfer from the bulk to a specific site on the surface, while basic groups on the surface will accelerate the dissipation of the proton to the bulk. This qualitative description is corroborated by accurate quantitative analysis based on experimentally determined rate constants.

There is hardly an enzyme-catalyzed reaction where the proton does not serve as a substrate, product, or intermediate. Thus, a rapid proton pulse can perturb most enzymic reactions through their interaction with the catalytic mechanism. Such perturbation is readily achieved by the laser-induced proton pulse (Gutman & Huppert, 1979), which can produce an intensive transinate acidification of aqueous solutions (10–50 μM H^+) within a few nanoseconds.

The application of this technique in enzymology is not straightforward due to the fact that the shape of the perturbing function is modulated by the reactants present in the solution (Gutman et al., 1983a,b; Gutman, 1984; Nachliel & Gutman, 1984). Because of that, any attempt to perturb the equilibrium of enzymes by a proton pulse and to measure the kinetics of the subsequent reaction will be hampered by the interaction of the protons with the rest of the proton binding sites in the solution (enzyme and substrate).

In the preceding paper (Gutman et al., 1985) we analyzed the effect of soluble buffer on the dynamics of protonation of a proton detector. In this paper we shall investigate the effect of buffer moieties carried by the same macromolecular body to which the proton detector is attached.

The model systems we selected for our studies are Brij 58 micelles carrying two pH indicators, bromocresol green and neutral red (Gutman et al., 1981; Nachliel & Gutman, 1984). In a previous study (Gutman et al., 1983b), we have measured the dynamics of protonation of each indicator when attached

† This research was supported by the American–Israel Binational Science Foundation, 3101/82.

0006-2960/85/0424-2941$01.50/0 © 1985 American Chemical Society

to these micelles. The absorption spectra of these two indicators are well distinguished of each other; thus, we can define one reactant as "indicator" and measure its kinetics, while the other will function as "buffer". Bromocresol green is used as indicator, while neutral red, which in its alkaline state is uncharged, is used as buffer. The two reactants, when adsorbed to the micelle, are located on the interface of the micelle and expose to the bulk phase a proton-detection surface of ~6 Å in diameter (Gutman et al., 1983b; Gutman, 1984).

The high affinity of neutral red to the micelle enabled us to vary its average occupancy on the micelle so that the ratio indicator/buffer could be varied at will. We find this system to be a very convenient model, as the micelles are homogeneous in size and practically uncharged and variable stoichiometry of reactants is readily achieved.

In this study we used the numerical solution of the differential rate equations (see preceding paper) to represent the dynamics of all reactants: the experimentally observed reactant (indicator) and the unobserved ones (free protons, buffer, and conjugate base of proton emitter). The validity of the mathematical presentation is demonstrated by the accurate reconstruction of the observed dynamics. This procedure expands our capacity to monitor the bulk to surface and surface to bulk proton flux. We shall demonstrate that, during the pulse experiment, the mechanism of proton flux varies with time. The protonation of macromolecule is dominated by the reaction of the free protons, while the relaxation to the prepulse state is established through collisional proton transfer between the conjugate base in the solution and Lewis acids on the macromolecule. Immobile buffer, adsorbed on the macromolecule surface, accelerates the reactions between specific sites with protons and soluble buffer in the bulk. Low-pK surface groups enhance the rate of protonation while high-pK buffer accelerates the deprotonation.

Materials and Methods

Reagents, instrumentation, and numerical solution of the coupled differential rate equations were as described in the preceding paper (Gutman et al., 1985). Brij 58 [poly(oxyethylene) 20 cetyl ether] was a Sigma product.

Results

Determination of Experimental Conditions. The distribution ratio of bromocresol green and neutral red between water and Brij 58 micelles has been determined according to Tong & Glesmann (1957). For the alkaline forms the values are 1100 ± 100 and 1400 ± 100, respectively. Thus in a solution containing 4% v/v of Brij 58, 96% of the dyes will be adsorbed on the micelles. This detergent concentration corresponds to 500 μM micelles. In order to have a homogeneous micelle population carrying one (average value) molecule of bromocresol green and a few molecules of neutral red, we added 500 μM bromocresol green and higher concentration of neutral red. Throughout this study we shall refer to the average occupancy number of each dye, disregarding the precise Poisson distribution.

Because of the high concentration of the indicator the reaction was carried out in a short (1-mm) optical path cell with collinear analyzing and excitation beams (Gutman, 1984). The high concentration of reactants results in a very fast velocity of protonation (Gutman, 1984). The reaction was so fast that even with a 20 ns/address time resolution of the transient recorder we could not satisfactorily resolve the signal rise time. Because of that we analyzed our experiments with only Y_{max} and γ_2 as accurate macroscopic parameters [for discussion see Gutman (1984)].

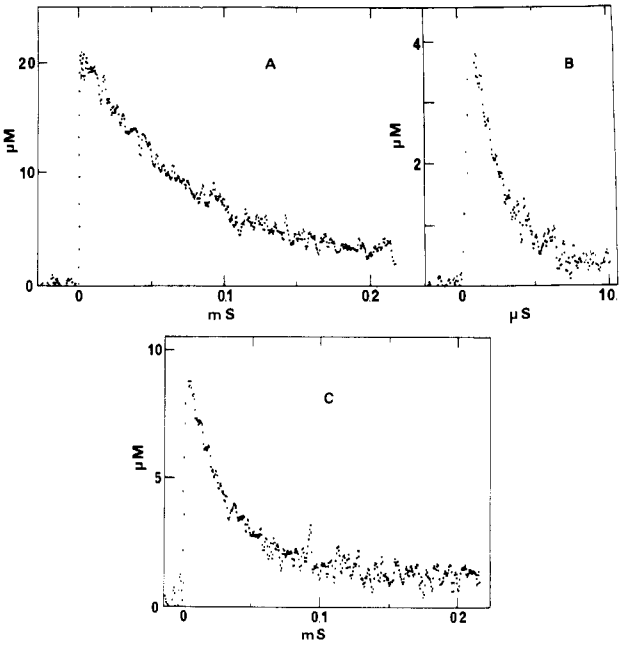

FIGURE 1: Dynamics of pulse protonation of bromocresol green adsorbed to Brij 58 micelles. The reaction was measured in the presence of 40 mg of Brij 58/mL (equivalent to 500 μM micellar concentrations), 500 μM bromocresol green, 1 mM proton emitter 2-naphthol-3,6-disulfonate, pH 7.5, and 10 mM NaCl. (Ordinate) Micromoles of indicator protonated by single pulse. (A) No further addition; (B) in the presence of 2 mM imidazole; (C) in the presence of 2.5 mM neutral red adsorbed in the micelles.

Pulse Protonation of Adsorbed Bromocresol Green in the Presence of Soluble Buffer (Imidazole). The transient protonation of adsorbed bromocresol green in the absence and the presence of 2 mM imidazole (pK = 7) is shown in Figure 1A,B. The reactions involved are summarized in eq 1–6.

$$ROH \underset{k_2}{\overset{k_1}{\rightleftharpoons}} RO^- + H^+ \quad (1)$$

$$HIn \underset{k_4}{\overset{k_3}{\rightleftharpoons}} In^- + H^+ \quad (2)$$

$$BH \underset{k_6}{\overset{k_5}{\rightleftharpoons}} B^- + H^+ \quad (3)$$

$$BH + In^- \underset{k_8}{\overset{k_7}{\rightleftharpoons}} B^- + HIn \quad (4)$$

$$BH + RO^- \underset{k_{10}}{\overset{k_9}{\rightleftharpoons}} ROH + B^- \quad (5)$$

$$HIn + RO^- \underset{k_{12}}{\overset{k_{11}}{\rightleftharpoons}} ROH + In^- \quad (6)$$

Of all rate constants appearing in these equations, we have already determined all but k_7 and k_{12}. These two values were determined by solving the differential rate equations corresponding with the experimental system (see preceding paper and its Appendix). These rate constants will generate, through the differential rate equation, a set of functions that will vary with the initial conditions exactly as the experimental results do. As seen in Figure 2, the rate constants we derived indeed simulate the dependence of the macroscopic parameters on the buffer concentration. The rate constants characterizing the reaction are listed in Table I, soluble buffer.

Effect of Micellar-Bound Buffer on Dynamic Protonation of Bromocresol Green. The experiment describe above was repeated at the same range of buffer concentrations with the hydrophobic indicator—neutral red. Like imidazole, neutral red is uncharged in its alkaline form and carries one positive charge in its acidic state. The dynamics of protonation of

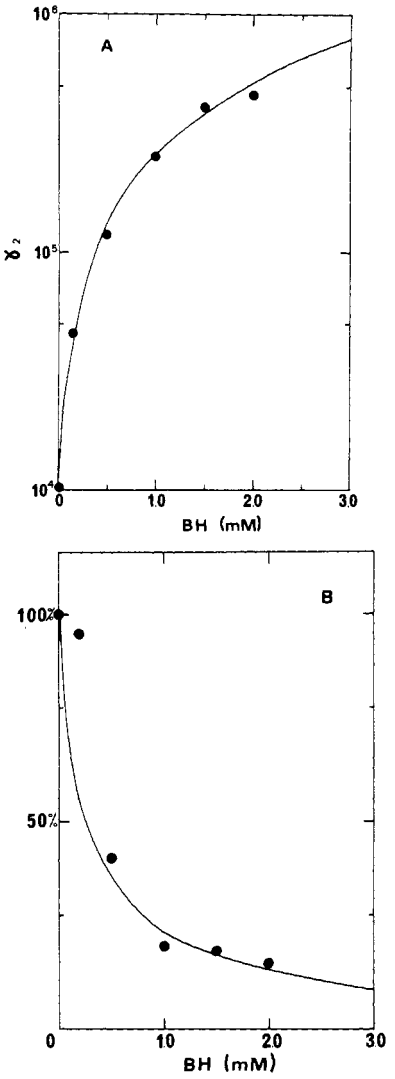

FIGURE 2: Dependence of the macroscopic parameters of the observed relaxation kinetics on the buffer concentration. The reaction was measured as in Figure 1A,B in the presence of the indicated imidazole concentrations. γ_2 was calculated as the first-order rate constant of the relaxation fitting the initial 60% of the relaxation. The lines drawn are the dependence of the same parameters characterizing computer-generated functions. These functions are the numerical solution of the differential rate equations describing the proton pulse events (see preceding paper). The rates corresponding to the lines are listed in Table I, soluble buffer. $X_0 = 35\ \mu M$. The concentrations of the reactants are identical with the experimental concentrations. (A) The variation of γ_2 as a function of imidazole concentration. (B) The variation of maximal amplitude (normalized for [buffer] = 0) vs. imidazole concentration.

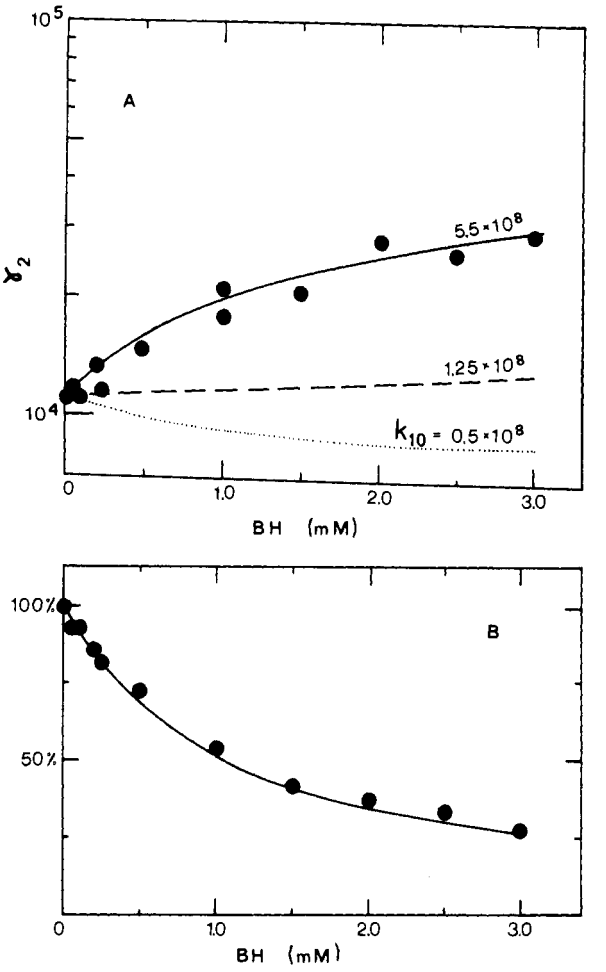

FIGURE 3: Dependence of the macroscopic parameters of the observed relaxation kinetics on the concentration of the micellar-adsorbed buffer. The reaction was measured as in Figure 1A,C with the indicated neutral red concentrations. The lines going through the experimental points were generated with the rate constants listed in Table I, immobile buffer. $X_0 = 35\ \mu M$. (A) The dependence of γ_2 on neutral red concentrations. The lines are drawn with varying values of k_{10} as indicated in the figure. (B) The dependence of maximal amplitude, normalized for [buffer] = 0.

bromocresol green adsorbed on micelles in the presence of neutral red is depicted in Figure 1C. The reaction was measured at 633 nm, a wavelength where the extinction coefficient of neutral red (50 M^{-1} cm^{-1}) is 3 orders of magnitude smaller than that of bromocresol green (3.3×10^4 M^{-1} cm^{-1}).

The dependence of the macroscopic parameters γ_2 and Y_{max} on the buffer concentrations is shown in Figure 3; the continuous lines are the theoretical predicted relationships as derived from the numerical solution of the differential rate equations with the rate constants listed in Table I, immobile buffer.

DISCUSSION

Model System. The purpose of this study was to evaluate the role of the buffering capacity of proteins on the dynamics of protonation of a specific site on their surface. For this reason we marked a micelle with two pH indicators of similar p*K*s and kinetic constants (Gutman et al., 1983b). One dye was "indicator" while the second functioned as a "buffer". The indicator dye, bromocresol green, has one negative charge in its protonated state ($BCG^{2-} + H^+ \rightarrow BCGH^-$), while the buffer dye, neutral red, is positively charged ($NR + H^+ \rightarrow NRH^+$). The initial conditions keep the buffer dye in its uncharged state (pH 7.5, $pK_{6,5} = 5.5$), which allows us to vary the micelle's dye content without affecting its charge. The perturbing proton pulse is small with respect to the micellar concentration (35 μM H^+ vs. 500 μM micelles), diminishing the probability of two protons reacting with the same micelle. This ensures that the charge increment of the protonated micelles is small (+1) and at [I] = 10 mM will have negligible effect on the system. The indicator dye, bromocresol green, can assume two configurations with respect to the micellar interface. The protonated bromocresol green reorients itself with respect to the micellar surface and inserts its proton bearing hydroxyl in the hydrophobic phase of the interface (Gutman et al., 1983b). The time constant of the post-protonation reorientation is $\tau = 700\ \mu s$. By limiting our analysis to a shorter time scale, less than 150 μs, we can exclude this reorientation event from our kinetic analysis.

Table I: Rate Constants of Partial Reactions Participating in Pulse Protonation of Bromocresol Green Adsorbed on Brij 58 Micelles in the Presence of Soluble or Micellar-Bound Buffer

rate constant (M^{-1} s^{-1})	buffer: soluble buffer (imidazole)[a]	buffer: immobile buffer (neutral red)[b]
k_1 (protonation of RO^-)	$(7.0 \pm 0.5) \times 10^{10}$	$(7 \pm 0.5) \times 10^{10}$
k_3 (protonation of In^-)	$(1 \pm 0.1) \times 10^{10}$	$(1 \pm 0.1) \times 10^{10}$
k_5 (protonation of buffer)	$(2 \pm 0.1) \times 10^{10}$	$(1 \pm 0.1) \times 10^{10}$
k_7 (collisional proton exchange between indicator and buffer, favorable direction)	$(4 \pm 0.7) \times 10^8$	$(1 \pm 0.2) \times 10^{10}$
k_{10} (collisional proton exchange between buffer and RO^-, favorable direction)	$(2.5 \pm 0.5) \times 10^9$	$(5.5 \pm 0.5) \times 10^8$
k_{12} (collisional proton exchange between indicator and RO^-, favorable direction)	1×10^8	1×10^8
$pK_{4,3}$ (pK of bound indicator)	5.35	5.55
$pK_{6,5}$ (pK of buffer)	7.0	5.45

[a] Measured at $I = 0.003$. [b] Measured at $I = 0.013$.

Effect of Soluble Buffer on Surface–Bulk Proton Transfer. The first section under Results demonstrates that the dynamics of protonation of micellar-bound bromocresol green is analyzable by the same differential equations written for the reaction between small free molecules (see preceding publication). The rate constants are listed in Table I. It is of interest to note that the rate constant for the reaction between the free reactants (RO^- or imidazole) with the micellar-bound indicator (k_7 and k_{12}, respectively) is only 2 orders of magnitude smaller than the reaction rate with free proton (k_1 and k_3, respectively). [The effects of interface and rotational diffusion on these rate constants were studied by Shoup et al. (1981), Weaver (1981), and Shoup & Szabo (1982).]

The 100-fold difference in rate constants implies that, in a solution where a protonable solute exceeds proton concentration more than 3 orders of magnitude, most of the proton flux will be mediated by the solute and not by proton diffusion. During the first nanoseconds, when 35 μM H^+ is ejected to the solution, they protonate any base they encounter, but once the free proton concentration decays to its prepulse level (3×10^{-8} M), the relaxation of the protonated bases is not carried out by proton dissociation–diffusion but through collisional proton exchange between them.

Effect of Surface-Bound Buffer on Dynamics of Proton Transfer. The role of buffer as proton carrier is also manifested when the buffer molecules are rigidily attached to the same carrier as the indicator. On a micelle carrying many protonable groups, a proton dissociating from one site has a high probability to encounter another conjugate base on the very same micelle. This high probability is reflected in the ultrafast rate constant of proton transfer between reactants located on the same micelle surface (Nachliel & Gutman, 1984). This effect is also demonstrated in Table I. The rate of proton transfer from micellar-bound bromocresol green to soluble, mobile imidazole is 4×10^8 M^{-1} s^{-1}. The reaction between the same indicator and neutral red, when adsorbed to the micelle, is much faster.

Effect of Collisional Proton Transfer. The rate constant of proton dissociation from the two adsorbed indicators (k_4 and k_6) is roughly the same, but the collisional proton transfer to RO^- renders NRH^+ to be a better proton exit port. As documented in Figure 3A, the rate of relaxation of protonated bromocresol green is accelerated by increasing the surface

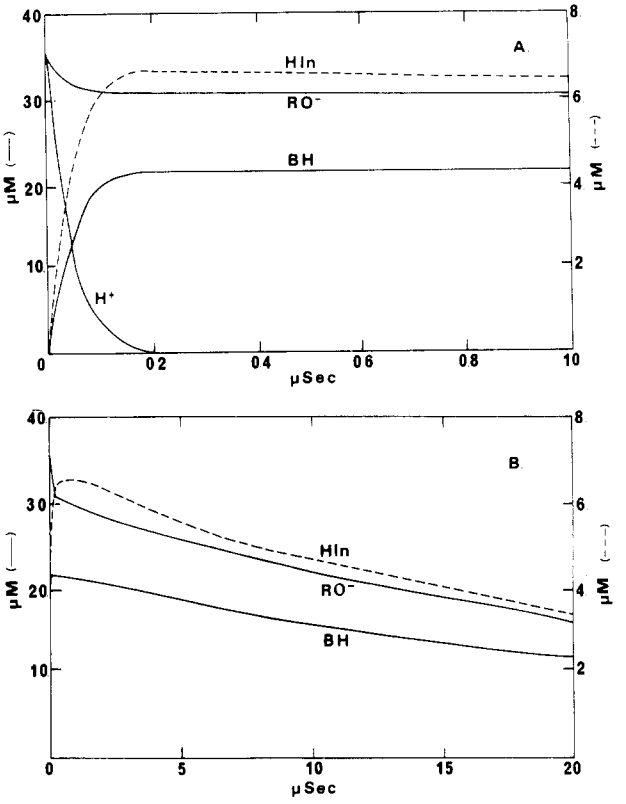

FIGURE 4: Computer simulation of the dynamics of all reactants participating in pulse protonation of bromocresol green adsorbed on micelles carrying immobile buffer moieties. The curves were generated with the rate constants listed in Table I, immobile buffer, with the following reactant concentrations: Bromocresol green, 500 μM; 2-naphthol-3,6-disulfonate, 1 mM; neutral red, 1.5 mM; pH 7.5; X_0 = 35 μM. (A) Simulation of the reaction during the first microsecond. (B) Simulation over 20 μs.

buffer content of the micelles. The line going through the experimental point is calculated for collisional proton transfer, $k_{10} = 5.5 \times 10^8$ M^{-1} s^{-1}. In this figure we also drew lines representing some hypothetical systems. In a case where buffer and site react with RO^- at the same rate, $k_{10} = k_{12} = 1.25 \times 10^8$ M^{-1} s^{-1}. The relaxation of the site (represented by the kinetic parameters of bromocresol green) is nearly unaffected by the buffer content. A slow reaction of buffer and RO^- reverses the shape of the line. The buffer serves as a slowly depleted proton reservoir and extended the life time of protons in the site (Figure 3A, $k = 0.5 \times 10^8$ M^{-1} s^{-1}).

Visualization of Buffer and Emitter Dynamics. The numerical solution of the differential rate equation is not only an instrument for determining the rate constants of the reactions. It also reconstructs the transients of all reactant concentrations. Using the kinetic parameters listed in Table I, immobile buffer, we generated dynamics of all reactants. Within 1 μs there is an extremely fast consumption of the free protons, with a time constant of 30–50 ns. As seen in Figure 4A, only a small fraction of the protons are recaptured by the RO^-. This fast phase ends with 80% of discharged protons attached to the micellar borne bases, while the bulk is enriched with RO^-. About 100 ns after the pulse, the free proton concentration is already negligible with respect to the other reactants. Thus, we can approximate

$$\Delta[RO^-]_t = \Delta[BCGH^-]_t + \Delta[NRH^+]_t$$

As the two species on the right side exchange protons at a very fast rate, a coupling between all reactants is achieved. Indeed, the three transients decay with the same time constant (Figure 4B). It is of interest to point out that the period where bulk

(RO^-) and surface (BCG and NR) are in disequilibrium is shorter than 100 ns (Figure 4A). If we accept this system as a model for bulk–surface proton transfer, then the local chemiosmatic theories describe an ultrashort lifetime phenomenon.

The rate-limiting step for the coupled relaxation of the three components is the proton transfer from the surface groups to the bulk phase. The time constant of the collisional proton transfer is given by $t = [(5.5 \times 10^8)([RO^-] + [NRH^+])]^{-1} = 30\ \mu s$. This time constant is comparable with that of proton dissociation from micellar-bound neutral red or bromocresol green ($k_6^{-1} \sim k_4^{-1} \sim 30\ \mu s$) (Gutman et al., 1983b). Of these two pathways the collisional mechanism is more efficient. Not every event of proton dissociation from surface group ends by protonation of RO^- in the bulk, while the collisional proton transfer (given by k_{10} or k_{12}) is the rate of the successful proton transfer. Figure 4 emphasizes a fundamental property of proton pulse experiments; the kinetic regime itself is time dependent. A very short time after the pulse when proton concentration is still high, the reaction is controlled by the proton diffusion. The fast consumption of protons diminishes the free proton flux until buffer diffusion controls the relaxation.

Two direct conclusions are based on these observations. (1) Macromolecular structures, in spite of their slow translational diffusion, are very efficient proton acceptors and compete effectively with small solutes [see Richter & Eigen (1974)]. (2) In buffered solutions the transfer of proton from the surface group of a macromolecule to the bulk is mostly carried out by the mobile buffer. In our particular case 30 μM disulfononaphtholate (analogous to a buffer in biochemical reactions) is sufficient to remove a proton from the micellar surface at a rate exceeding the dissociation–diffusion pathway. As seen in Figure 2A, 500 μM imidazole suffices to accelerate surface deprotonation by 1 order of magnitude.

Using these results, we can deduce that even a low concentration of soluble proton carriers (ATP, ADP, P_i, etc.) will suffice to remove a proton from protogenic surfaces like mitochondria, bacterial chromatophores, thylakoid membranes, etc. at a rate exceeding the spontaneous dissociation.

Effect of Rate Constants on Dynamics of Bulk–Surface Proton Transfer. Figure 5 demonstrates the dependence of Y_{max} and γ_2 on the rate constants for three hypothetical cases. Line a was computed for a system where both site and buffer react with RO^- at rate constants slower than the spontaneous dissociation of the buffer: $k_6 > k_{10}[RO^-]$ and $k_{12}[RO^-]$. In such a case the rate of surface proton exchange (k_7) hardly affects the deprotonation of the site but supports its protonation (as indicated by the increased amplitude at high values of k_7). Any proton that encounters a surface group will have a higher probability of reaching the site of interest through the fast proton exchange between surface groups (Nachliel & Gutman, 1984).

In the case where the surface buffer reacts with RO^- faster than the site (as in our model system), the rate of the observed deprotonation will increase with k_7 (Figure 5A, line b); it assists in dissipating the proton from the macromolecule surface. The surface buffer still acts as proton acceptor with respect to the bulk. But as it also serves as the major proton exit port, higher values of k_7 are needed to exploit its full capacity to serve as proton guide (Figure 5B, line b). Line c in Figure 5A depicts the characteristics of an opposite case, where the site loses its proton to the mobile buffer faster than other surface groups (that would have been the state if we reversed the notation "buffer" and "indicator" in our system).

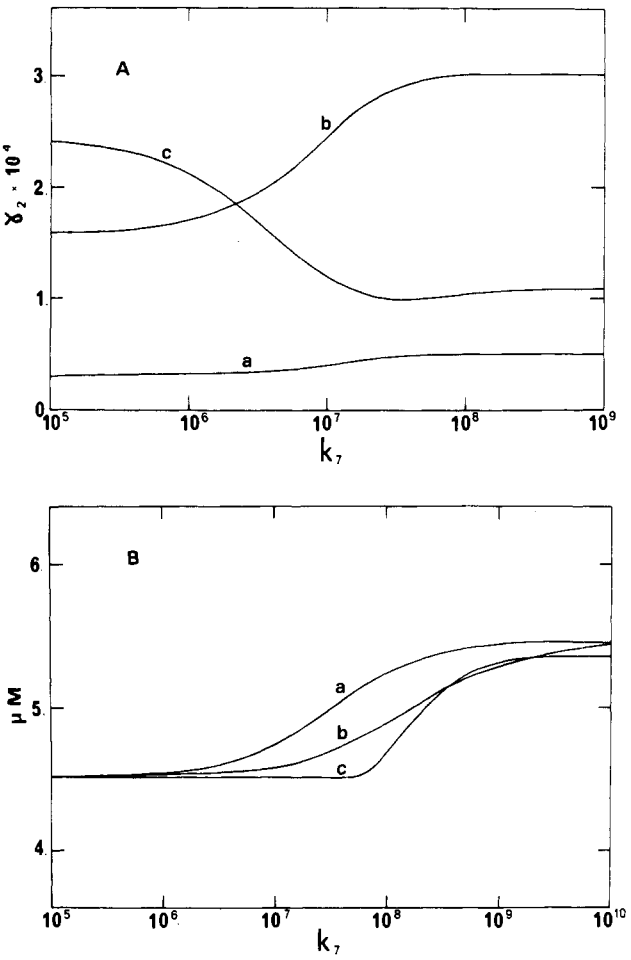

FIGURE 5: Dependence of γ_2 and maximal amplitude on the rate of proton exchange between surface groups. The parameters γ_2 and HIn_{max} were calculated from computer-generated curves describing the reaction taking place in a system consisting of 500 μM micelles each carrying (average value) one proton detector, represented by the kinetic parameters of bromocresol green and six buffer molecules characterized by k_5 of neutral red in the presence of 1 mM proton emitter (2-naphthol-3,6-disulfonate). The rates k_7, k_{10}, and k_{12} were set as given in the figures. (Line a) $k_{10} = 5.5 \times 10^5\ M^{-1}\ s^{-1}$; $k_{12} = 1 \times 10^7\ M^{-1}\ s^{-1}$. (Line b) $k_{10} = 1 \times 10^7\ M^{-1}\ s^{-1}$; $k_{12} = 5.5 \times 10^8\ M^{-1}\ s^{-1}$. (Line c) $k_{10} = 5.5 \times 10^8\ M^{-1}\ s^{-1}$; $k_{12} = 5.5 \times 10^6\ M^{-1}\ s^{-1}$. (Frame A) γ_2 vs. k_7. (Frame B) HIn_{max} vs. k_7.

The fast surface proton transfer in this case serves to shelter the protons in less reactive sites. The surface buffer groups act as proton reservoir, reprotonating the site of interest whenever it loses its proton to the bulk. As the site of interest is the major proton exit port, very high surface proton flux is needed to reach the maximal level of its protonation (Figure 5B, line c).

The fast proton flux between adjacent surface groups is attributed to the small distance between them (Nachliel & Gutman, 1984). As tight packing of protonable groups is common in proteins, phospholipid membranes, and nucleic acids, we can assume that most biomolecules of interest will fall in the regime of fast proton flux between surface groups, i.e., at the right side of Figure 5. Still, due to the heterogeneity of protein surfaces and their structural complexities, secluded sites on proteins are recognized, characterized by their very slow equilibration with the bulk (or the rest of the protein) (Ugrabil & Bersohn, 1977; June et al., 1981; March et al., 1982). In the rest of our discussion we shall consider only the exposed sites.

To evaluate the role of surface groups' pK on the dynamics of protonation of a site of interest, we simulated a protonation

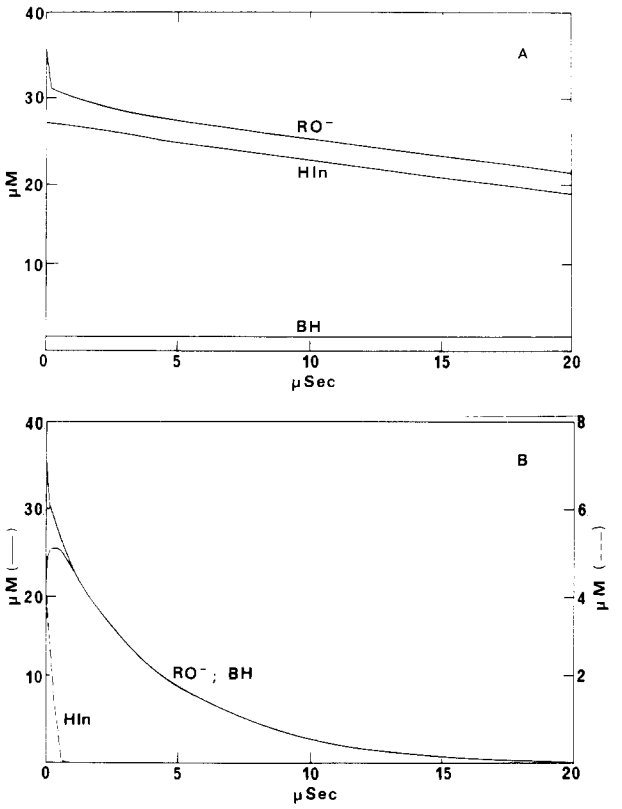

FIGURE 6: Computer simulation of the dynamics of all reactants participating in pulse protonation of proton detector [adsorbed on micelle carrying immobile buffer with pK = 4 (A) or pK = 7 (B)]. The curves were generated as described in Figure 4 only that the pK of the immobile buffer was set at the indicated values.

of a macromolecule carrying a single bromocresol green (site) and six buffer moieties with a pK of either 4 or 7. Figure 6A describes the dynamics generated for acidic buffer ($pK_{6,5}$ = 4.0). Within 100 ns after the perturbation (not shown), the free proton concentration has diminished the prepulse level, leaving the macromolecule protonated and the bulk enriched with RO^-. The fast proton transfer between the surface group distributes the protons according to the pK of the bases. As the site of interest is the strongest surface base, it retains 80% of the protons, though its molar ratio is 1:6 with respect to the immobile buffer. This demonstrates how acidic groups function as proton antenna, collecting and shuttling protons to more basic surface moieties.

Figure 6B depicts the course of events if the immobile buffer is more basic than the site of interest. Being the strongest surface base, and in high molecular excess, practically all protons are gathered by the surface buffer, and the site is rapidly deprotonated, discharging its protons to the bulk through the basic surface groups.

On the basis of this model system, we can assume that acidic moieties, with low pK, will mostly serve as receiving proton antennas. Whenever they encounter a free proton in the solution, they will be protonated for a very brief time [in accord with the low pK (Gutman, 1984)]. When the proton is released, it will have a high probability to react with another surface group. Thus, by fast hopping from one surface group to another (represented by the fast k_7) the proton will finally collide with the active site of the protein (the physiological target of the proton). Carboxylic acids on a protein or phospho head groups on a phospholipid will effectively collect free protons from the bathing solution. On the other hand, slightly alkaline side chains (histidines) will function mostly as "proton-transmitting antenna", accelerating the deprotonation of the site of interest. Consequently, our kinetic data indicate that the mechanism of a proton flux between bulk and a specific site on a protein might follow different pathways for protonation and deprotonation.

Registry No. Brij 58, 9004-95-9; bromocresol green, 76-60-8; 2-naphthol-3,6-disulfonate, 148-75-4; imidazole, 288-32-4; neutral red, 553-24-2.

REFERENCES

Bersohn, R. (1980) in *Molecular Structure and Dynamics* (Balaban, M., Ed.) pp 269–278, International Science Service.

Gutman, M. (1984) *Methods Biochem. Anal. 30*, 1–103.

Gutman, M., & Huppert, D. (1970) *J. Biochim. Biophys. Methods 1*, 9–19.

Gutman, M., Huppert, D., Pines, E., & Nachliel, E. (1981) *Biochim. Biophys. Acta 642*, 15–26.

Gutman, M., Nachliel, E., Gershon, E., Giniger, R., & Pines, E. (1983a) *J. Am. Chem. Soc. 105*, 2210–2216.

Gutman, M., Nachliel, E., Gershon, E., & Giniger, R. (1983b) *Eur. J. Biochem. 134*, 63–69.

Gutman, M., Nachliel, E., & Gershon, E. (1985) *Biochemistry* (preceding paper in this issue).

Jonsson, B. H., Steinor, H., & Linkskeg, S. (1976) *FEBS Lett. 64*, 310–314.

June, D. S., Saelter, C. H., & Dye, J. L. (1981) *Biochemistry 20*, 2707–2719.

March, K. L., Maskalick, D. G., England, R. D., Friend, S. H., & Gard, F. R. N. (1982) *Biochemistry 21*, 5241–5251.

Nachliel, E., & Gutman, M. (1984) *Eur. J. Biochem. 143*, 83–89.

Richter, P. H., & Eigen, M. (1974) *Biophys. Chem. 2*, 255–263.

Shoup, D., & Szabo, A. (1982) *Biophys. J. 40*, 33–39.

Shoup, D., Lipari, G., & Szabo, A. (1981) *Biophys. J. 36*, 697–714.

Silvestrini, M. C., Brunori, M., Wilson, M. T., & Darley-Usmar, V. M. (1981) *J. Inorg. Chem. 14*, 327–338.

Tong, L. K. J., & Glesmann, M. C. (1957) *J. Am. Chem. Soc. 79*, 4305–4309.

Ugurbil, K., & Bersohn, R. (1977) *Biochemistry 16*, 3016–3023.

Weaver, D. L. (1983) *Biophys. J. 41*, 81–86.